



Contents lists available at ScienceDirect

Journal of Pharmaceutical and Biomedical Analysis

journal homepage: www.elsevier.com/locate/jpba



Determination of motolimod concentration in rat plasma by liquid chromatography-tandem mass spectrometry and its application in a pharmacokinetic study

Yu-Geun Ji^{a,1}, Yu-Mi Shin^{a,1}, Jong-Woo Jeong^a, Hae-In Choi^a, Seung-Won Lee^a,
Jong-Hwa Lee^b, Kyeong-Ryoon Lee^{c,*}, Tae-Sung Koo^{a,*}

^a Graduate School of New Drug Discovery and Development, Chungnam National University, 99 Daehak-ro, Yuseong-gu, Daejeon 34134, Republic of Korea

^b DMPK Group, Korea Institute of Toxicology, 141 Gajeong-ro, Yuseong-gu, Daejeon 34114, South Korea

^c Laboratory Animal Resource Center, Korea Research Institute of Bioscience and Biotechnology, 30 Yeongudanji-ro, Ochang, Republic of Korea

ARTICLE INFO

Article history:

Received 18 July 2019

Received in revised form 4 November 2019

Accepted 11 November 2019

Available online xxx

Keywords:

VTX-2337

Liquid chromatography-tandem mass spectrometry

Pharmacokinetics

Toll-like receptor 8

ABSTRACT

Motolimod (VTX-2337) is an agonist of toll-like receptor 8. In this study, a novel and sensitive liquid chromatography-tandem mass spectrometry method was developed for quantifying motolimod in rat plasma and subsequently used in a pharmacokinetic study. Proteins were precipitated from plasma samples using acetonitrile prior to the analysis. GS-9620 was used as an internal standard. High-performance liquid chromatography was performed using a Spursil C18-EP column (3 μ m, 50 \times 2.1 mm). Aqueous ammonium formate and acetonitrile were used as the mobile phase. Motolimod was detected using an electrospray ionization interface under multiple reaction monitoring conditions in the positive ion mode. The developed method produced a linear correlation over a concentration range of 1–1000 ng/mL ($r = 0.9944$). Intra- and inter-day precision values ranged from 4.8%–10.7% (the lower limit of quantification precision value was 16.3 %), whereas intra- and inter-day accuracy values ranged from 0.3%–9.1 %. The mean recovery of motolimod from rat plasma was 109.4 %. Additionally, motolimod was found to be stable under various conditions (three freeze-thaw cycles, 6-h storage at room temperature, short- and long-term stability tests, and processing). The developed method was successfully used in a pharmacokinetic study in rats. Motolimod showed non-linear pharmacokinetics following its intravenous administration to rats at 0.6–6 mg/kg. Additionally, very low exposure (<1 %) was obtained following oral administration of the drug to rats. The results also showed that motolimod has a low metabolic stability in the liver microsomes and exhibits extensive binding to the plasma proteins.

© 2019 Elsevier B.V. All rights reserved.

Abbreviations: AUC, area under the plasma concentration-time curve; CL, systemic clearance; CL_h, hepatic clearance; CL_{int}, *in vitro*, microsomal intrinsic clearance; CL_{u, int}, *vivo*, unbound hepatic intrinsic clearance; C_{max}, peak plasma concentration; CYP, cytochrome P450; DMSO, dimethyl sulfoxide; f_{u, mic}, microsome-unbound fraction of motolimod; f_{ub}, blood-unbound fraction of motolimod; k_e, metabolic rate constant; LC-MS/MS, liquid chromatography-tandem mass spectrometry; NC, not calculated; QC, quality control; RSD, relative standard deviation; ssRNA, single-stranded RNA; T_{1/2}, terminal elimination half-life; TLR, toll-like receptor; T_{max}, time to reach C_{max}; V_{ss}, steady-state volume of distribution.

* Corresponding authors.

E-mail addresses: kyeongrlee@kribb.re.kr (K.-R. Lee), kootae@cnu.ac.kr (T.-S. Koo).

(T.-S. Koo).

¹ These authors contributed equally to this work.

1. Introduction

Toll-like receptor (TLR) is a family of pathogen recognition receptors in the human body distributed on and inside dendritic cells, macrophages, and natural killer cells. Activation of TLR leads to immune responses and cytokine secretion, and thereby, activates the adaptive immunity [1]. TLR8 is a natural ligand for viral single-stranded RNA (ssRNA) and has recently been shown to stimulate the release of tumor necrosis factor- α by recognizing the ssRNA produced by HIV-1 [2]. Therefore, TLR8 contributes to adaptive immunity in many ways, which include the activation of antitumor T cells [3]. Motolimod (VTX-2337) is a small molecule that was developed at Array BioPharma (Boulder, USA) and is licensed for production by VentiRx Pharmaceuticals (Seattle, WA, USA). As a TLR8 agonist, it is known to increase the antibody-dependent cell-mediated cytotoxicity response by activating the natural killer

<https://doi.org/10.1016/j.jpba.2019.112987>

0731-7085/© 2019 Elsevier B.V. All rights reserved.

Please cite this article as: Y.-G. Ji, Y.-M. Shin, J.-W. Jeong et al., Determination of motolimod concentration in rat plasma by liquid chromatography-tandem mass spectrometry and its application in a pharmacokinetic study, J. Pharm. Biomed. Anal., <https://doi.org/10.1016/j.jpba.2019.112987>

cells, monocytes, and dendritic cells. Recently, phase 1 and phase 2 clinical trials on motolimod for the treatment of ovarian and head and neck cancers have been completed in the United States. In the phase 1 study, it was found that motolimod could induce a positive immune response. In the phase 2 trial, a combination therapy with motolimod and cetuximab did not improve the survival of patients with recurrent and/or metastatic squamous cell carcinoma of the head and neck. However, the results for a pre-specified subgroup revealed that motolimod significantly prolonged the survival outcomes among patients who were human papillomavirus (HPV)-positive, which suggests that further evaluation of HPV-positive parietal cancer is essential [4].

There are many reports on the pharmacological effects of motolimod as well as on the clinical outcomes observed after treatment with motolimod; however, reports on the pharmacokinetic properties of motolimod are limited. Recently, a study on the metabolism of motolimod in liver microsomes indicated that a metabolite formed by depropylation was the most abundant metabolite. Additionally, the results showed that the metabolism of motolimod is similar in rats and humans [5]. In that paper, a method for determining the concentration of motolimod in microsomes using Orbitrap mass spectrometry, which is generally used for qualitative analysis, was reported. However, this method is unreliable because it does not provide validation information, including quantification range, accuracy, and precision.

Despite the abundance of studies on motolimod, information about the quantitative bioanalysis of motolimod in plasma samples is not available. Also, there is very limited information about pharmacokinetics of experimental animals, especially rat, generally used as reference data, although a thorough understanding of how a reference drug functions is essential in modern drug discovery studies. In this study, we developed and validated a reliable liquid chromatography-tandem mass spectrometry (LC-MS/MS) method for measuring the motolimod levels in rat plasma. The method was then used in a pharmacokinetic study of motolimod in rats.

2. Material and methods

2.1. Materials

Motolimod ($\geq 98\%$ purity) and GS-9620 (internal standard) were purchased from Selleck Chemicals (Houston, TX, USA) and AdooQ Bioscience (Irvine, CA, USA), respectively. Dimethyl sulfoxide (DMSO) and ammonium formate were purchased from Sigma-Aldrich (St. Louis, MO, USA) and Junsei Chemical Co. Ltd. (Tokyo, Japan), respectively. Acetonitrile (high-performance liquid chromatography [HPLC] grade) and methanol (HPLC grade) were obtained from J. T. Baker Chemicals (Phillipsburg, NJ, USA). Hydrochloric acid was obtained from Matsuno Chemicals Ltd. (Osaka, Japan). Ethyl acetate was obtained from Samchun Chemical (Pyeongtaek, Korea). All other chemicals used were either of HPLC grade or of the highest grade available. The rat plasma containing sodium heparin as an anticoagulant was prepared in our laboratory and used as blank.

2.2. Liquid chromatography and mass spectrometry

Samples were analyzed using an Agilent 1100 HPLC system (Agilent Technologies, Santa Clara, CA, USA) and an API 4000 mass spectrometer (Applied Biosystems Inc., Foster City, CA, USA). Chromatographic separation was performed using ammonium formate (40 mM)-acetonitrile (30:70, v/v) as the mobile phase on a Spursil C18-EP column (3 μm , 50 \times 2.1 mm; Dikma Technologies Inc., Lake Forest, CA, USA). The flow rate of the mobile phase was set at 0.3 mL/min and the injection volume was 5 μL . The mass spectrom-

etry parameters were as follows: ion voltage, 5500 V; temperature, 600 $^{\circ}\text{C}$; curtain gas, 20 psi; nebulizer gas, 50 psi; turbo gas, 60 psi; entrance potential, 11 V; declustering potential, 71 and 106 V; collision energy, 39 and 49 V; and collision cell exit potential, 20 and 8 V for motolimod and GS-9620, respectively. The multiple reaction mode transitions were m/z 459.22 \rightarrow 330.40 for motolimod and m/z 411.30 \rightarrow 105.20 for GS-9620.

2.3. Sample preparation

The aliquots, 50 μL of rat plasma and 50 μL of GS-9620 solution (200 ng/mL), were transferred into microcentrifuge tubes (Axygen, Union City, CA, USA). Plasma proteins were precipitated by adding 100 μL of acetonitrile, followed by vortexing of the mixture for 10 min. The mixture was then centrifuged at 17,600 \times g for 10 min and the supernatant was transferred into a vial [6].

2.4. Method validation

The following parameters were investigated based on the guidelines set by the United States Food and Drug Administration and the European Medicines Agency: selectivity, linearity, precision, accuracy, matrix effect, recovery, process efficiency, and stability [7,8].

The selectivity of the method was evaluated by comparing the results obtained for blank plasma samples from six Sprague-Dawley (SD) rats, blank plasma spiked with motolimod working solution and GS-9620, and a plasma sample taken 45 min after motolimod administration. Retention times were compared to ensure the absence of interference from unpurified endogenous substances, denaturing agents, or other compounds, in accordance with the guidelines named above. Calibration curves for motolimod present in the rat plasma were obtained by plotting the peak ratios of motolimod to GS-9620 versus the nominal concentrations of motolimod calibration standards (1, 2, 5, 10, 30, 300, 600, and 1000 ng/mL). The calibration curves were fitted using a linear least-squares regression with a weighting factor of $1/x^2$.

Intra- and inter-day precision and accuracy were evaluated by analyzing six replicate quality control (QC) samples at different concentrations (1, 3, 100, and 900 ng/mL) on the same day and on three consecutive days, respectively. Relative standard deviation (RSD) and relative error values were used to estimate the precision and accuracy, respectively. The criteria for data acceptance were that accuracy was within $\pm 15\%$ of the standard deviation from the nominal values and precision was within $\pm 15\%$ of the RSD. The acceptance criteria for the lower limit of quantification (LLOQ) were that the precision and accuracy values were $< 20\%$ of the RSD and 20% of the RE, respectively. Six different sources of plasma were used for each group of replicate samples.

Matrix effect, recovery, and process efficiency were examined based on purification. Four repeated measurements were performed for one sample from each of the QC levels (3, 100, and 900 ng/mL), after which QC sets were established. Set 1 was defined as the mean peak area for motolimod and GS-9620 in the mobile phase, set 2 was defined as the mean peak area of motolimod and GS-9620 spiked in the extract of the blank plasma, and set 3 was defined as the mean peak area of motolimod and GS-9620 in the plasma. The matrix effect was evaluated by comparing the peak area responses in set 2 with those in set 1 at the same concentrations. Purification recovery was validated by comparing the peak area responses in set 3 with those in set 2. The process efficiency was determined by comparing the data in set 3 with those in set 1 [9,10].

The stability of motolimod in plasma was evaluated by determining the amounts of motolimod in QC samples (3 and 900 ng/mL) after three freeze-thaw cycles at -20°C , storage at room temper-

ature for 6 h prior to treatment, and storage at -20°C for 28 days. The processed sample stability was determined to investigate the stability of processed samples in an autosampler. This was done by assessing the QC samples and stock solutions in four replicates.

2.5. Pharmacokinetic studies

Male SD rats (7-weeks old) weighing 180–240 g were purchased from Orient Bio (Seongnam, Korea). The animals were kept in plastic cages under the following conditions: 12/12 h light/dark cycle; temperature, $20\text{--}25^{\circ}\text{C}$; and relative humidity, 40–60 %. The rats were not given food for 14 h prior to dose administration; however, they were allowed free access to water. After dosing, no food or water was allowed for a further 4 h. The experimental protocols were reviewed by the Institutional Animal Care and Use Committee of Chungnam National University (CNU-00972; Daejeon, Korea).

Motolimod was dissolved in a mixture of 10 % DMSO, 20 % 0.05 N HCl, and 70 % saline and administered to the rats ($n=5$) as an intravenous bolus (0.6, 2, or 6 mg/kg) via the tail vein or by oral gavage (0.6 mg/kg). The dosing volume was 2 mL/kg. Blood samples (150 μL) from the jugular vein were collected in heparinized tubes at 0.05 (intravenous only), 0.12, 0.25, 0.5, 0.75, 1, 2, 3, 5, and 7 h after dosing. All blood samples were centrifuged at $17,600 \times g$ for 10 min to obtain the plasma, which was then frozen at -20°C until the analyses.

The pharmacokinetic parameters were determined by analyzing the plasma concentration-time profiles using a non-compartmental method. Because non-linear pharmacokinetics were observed in this study [11], we analyzed it using compartmental analysis with non-linear kinetics, as well, as shown in the following equations.

$$\frac{dC_1}{dt} = -k_{12} \cdot C_1 + k_{21} \cdot C_2 - \frac{V_{max} \cdot C_1}{K_m + C_1} \quad (1)$$

$$\frac{dC_2}{dt} = k_{12} \cdot C_1 - k_{21} \cdot C_2 \quad (2)$$

Where, C_1 and C_2 are the concentrations of central (i.e., the plasma concentrations) and peripheral compartments, respectively. k_{12} and k_{21} are the mass transfer rate constants of the drug from the central to the peripheral compartment and from the peripheral to the central compartment, respectively. K_m and V_{max} represent the Michaelis–Menten parameter and the maximal velocity of the non-linear elimination from the central compartment, respectively. All pharmacokinetic analyses in this study were performed using Phoenix WinNonlin 5.3. (Pharsight, St. Louis, MO, USA).

The metabolic stability of motolimod was evaluated using rat liver microsomes (BD Biosciences, San Jose, CA, USA). First, motolimod was dissolved in methanol at concentrations of 1, 3, 10, 30, 100, 300, 1000, and 3000 μM . Next, a 6.3- μL aliquot of rat liver microsomes (final concentration of protein, 0.5 mg/mL) was added to 226.5 μL of 0.1 M potassium phosphate buffer, after which the mixture was pre-incubated in a water bath at 37°C for 5 min. Afterwards, 2.5 μL of motolimod stock solution (final concentration of motolimod = 0.01, 0.03, 0.1, 0.3, 1, 3, 10, or 30 μM) and reduced nicotinamide adenine dinucleotide phosphate regeneration system solution were added to the mixture to activate the reaction. Aliquots of the resulting mixture were taken at 0, 3, 5, 7, 15, and 30 min after incubation in a shaking water bath (37°C , 90 rpm) for analysis. The reaction was stopped by adding 100 μL of cold acetonitrile to each sample [12]. The samples were then treated and quantitatively analyzed by LC–MS/MS. The concentration of motolimod remaining in each sample was plotted against time to calculate the metabolic rate constant (k_e) for each concentration. The elimination half-life ($T_{1/2}$), microsomal intrinsic clearance ($CL_{int, vitro}$), unbound hepatic intrinsic clearance ($CL_{u, int,$

$vivo$), and hepatic clearance (CL_h) were calculated using the following equations [13]:

$$T_{1/2} = -\ln 2 / k_e \quad (3)$$

$$CL_{int, vitro} = k_e \times (\text{mL incubation} / \text{mg microsomes}) \quad (4)$$

$$CL_{u, int, vivo} = f_{u, mic} \times CL_{int, vitro} \times (45 \text{ mg microsomes} / \text{g liver}) \times (\text{g liver} / \text{kg b.w.}) \quad (5)$$

$$CL_h = f_{ub} \times CL_{u, int, vivo} \times Q_h / (f_{ub} \times CL_{u, int, vivo} + Q_h) \quad (6)$$

$f_{u, mic}$ and f_{ub} in Eqs. (5) and (6) represent microsomal- and blood-unbound fraction of motolimod, respectively. The plasma-unbound fraction (f_u) was divided by the plasma to blood ratio (C_B/C_P) of motolimod to obtain f_{ub} . The liver weight and blood flow rate were 40 g/kg and 55 mL/min/kg, respectively [14].

An equilibrium dialysis machine (RED®; Thermo Fisher Scientific, Carlsbad, CA, USA) was used to investigate the binding of motolimod to plasma proteins and liver microsomes. Binding ratios were calculated according to Eq. (7). The chambers in the dialysis instrument were separated using semipermeable membranes, with the plasma or microsomal mixture containing motolimod in one chamber and phosphate buffer (pH 7.4) in the other chamber. Incubation was carried out in a shaking water bath at 37°C for 4 h at 100 rpm. Thereafter, acetonitrile was added to the mixture, followed by quantitative analysis by LC–MS/MS.

$$\text{Binding ratio} = 1 - (\text{concentration in buffer} / \text{concentration in plasma or microsomal mixture}) \quad (7)$$

2.6. Statistics

All data were expressed as means \pm SDs. Statistical analyses were performed via one-way analysis of variance (ANOVA) with Tukey's test or unpaired t -test using GraphPad Prism 7.03 (GraphPad Software Inc., La Jolla, CA, USA). The results were considered statistically significant at p values < 0.05 .

3. Results and discussion

3.1. Development of LC–MS/MS method

The mass spectrometry parameters were optimized to detect the most sensitive and stable protonated and product ions. The protonated molecular ions of motolimod and GS-9620 ($[M+H]^+$) were detected at m/z 459.22 and 411.30, respectively, by positive electrospray ionization in Q1 scan mode. In the initial product ion scan, the highest peak was at m/z 381.2; however, in the optimization process, the ion at m/z 330.4 was detected as the predominant ion. These results were reproducible when the mass spectrometer was connected to the HPLC. The product ions of motolimod and GS-9620 were detected using multiple reaction monitoring conditions at m/z 459.22 \rightarrow 330.40 and 411.23 \rightarrow 105.20, respectively (Fig. 1).

The peak shapes in the HPLC analysis were optimized using ZORBAX Eclipse XDB-C8, -C18, and -phenyl columns (Agilent Technologies) and mobile phases, such as formic acid and ammonium acetate buffer. However, poor peak shapes, such as peak tailing and fronting, could not be improved. It was considered that the N atom in the molecular structure of motolimod was affected by Si–OH on the column surface, which resulted in peak tailing; hence, an optimized peak could be obtained by high carbon loading [15]. Therefore, a Spursil C18-EP column (carbon loading 24 %), which

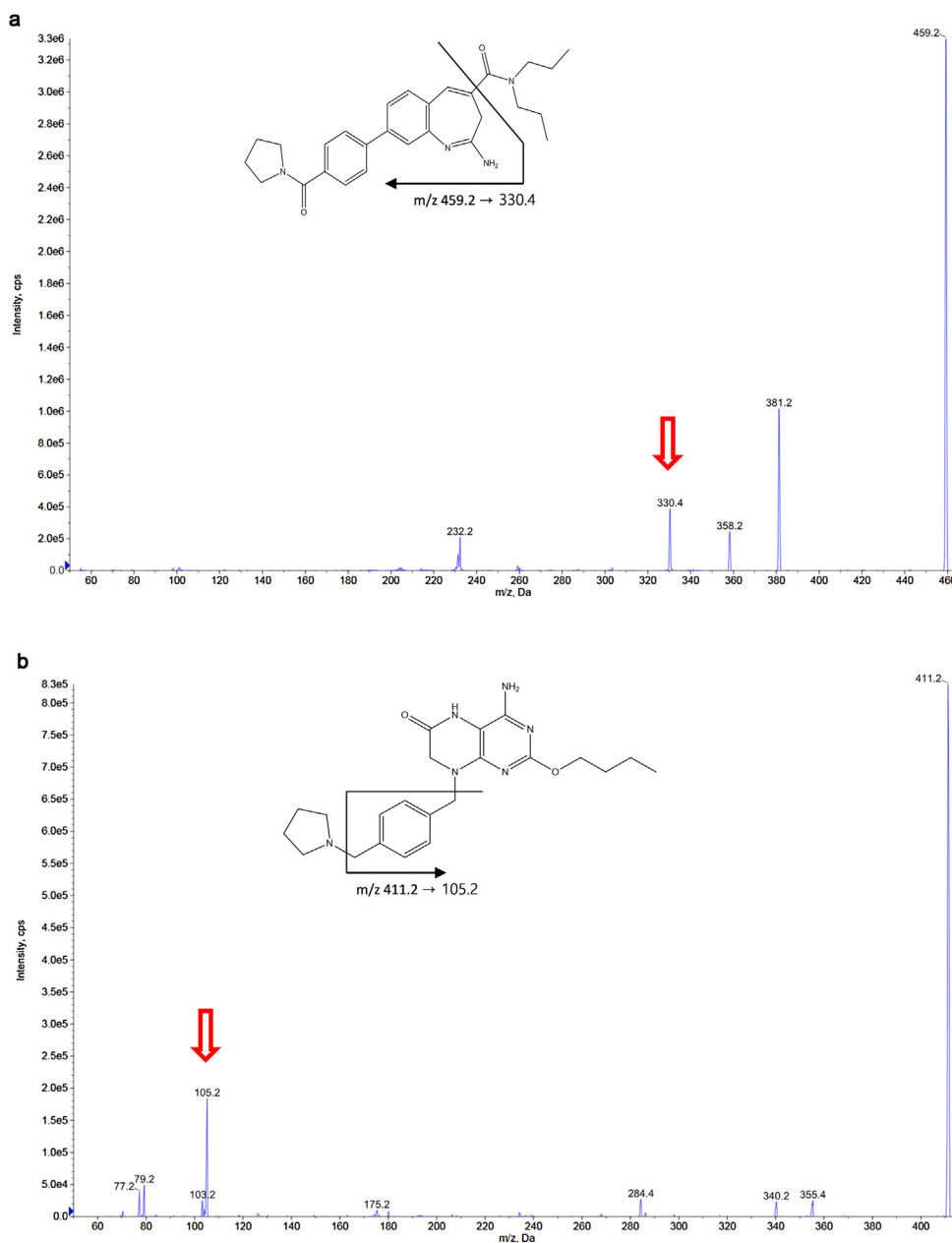


Fig. 1. Product ion mass spectra of (A) motolimod and (B) GS-9620.

has a higher carbon loading than the XDB-C8, -C18, and -phenyl columns (7.6, 10, and 7.2 % respectively), was used in the subsequent studies.

The optimized peak intensity and symmetry were obtained using the Spursil C18-EP column and ammonium formate (40 mM)-acetonitrile (30:70, v/v) as the mobile phase. It was noted that the carry-over phenomenon occurred when motolimod concentration was > 2000 ng/mL; therefore, the concentrations used were 1, 2, 5, 10, 30, 300, 600, and 1000 ng/mL.

3.2. Method validation

No interfering peaks were observed at 0.74 and 0.61 min, which were the retention times for motolimod and GS-9620, respectively. At the LLOQ level of 1 ng/mL for motolimod, the peak signal was at least five-fold higher than the baseline noise. The chromatograms for the double blank sample (without the analyte or GS-9620), blank sample (with GS-9620 only), LLOQ (1 ng/mL), and plasma samples

taken after intravenous injection of motolimod to rats are shown in Fig. 2.

The calibration curves for motolimod were plotted using six individual sources of double blank, blank, and calibration standard (1, 2, 5, 10, 30, 300, 600, and 1000 ng/mL) samples. The equation for the standard curve for motolimod that was obtained using a weighting factor of $1/x^2$ was $y = ax + b$ ($a = 0.00168$, $b = 0.00238$, $r = 0.9944$).

The intra- and inter-day precision and accuracy were evaluated using the LLOQ and three QC samples on the same day and on three different days. The results are summarized in Table 1. The intra- and inter-day precision and accuracy values ranged from 4.8%–16.3 % and 0.3%–9.1%, respectively. The results satisfied all the criteria and proved the reliability of the developed method.

The matrix effect, recovery, and process efficiency were estimated using the QC samples with concentrations of 3 and 900 ng/mL. The matrix effects of motolimod and GS-9620 in rat plasma were 94.3 % and 104.2 %, respectively. The recovery values

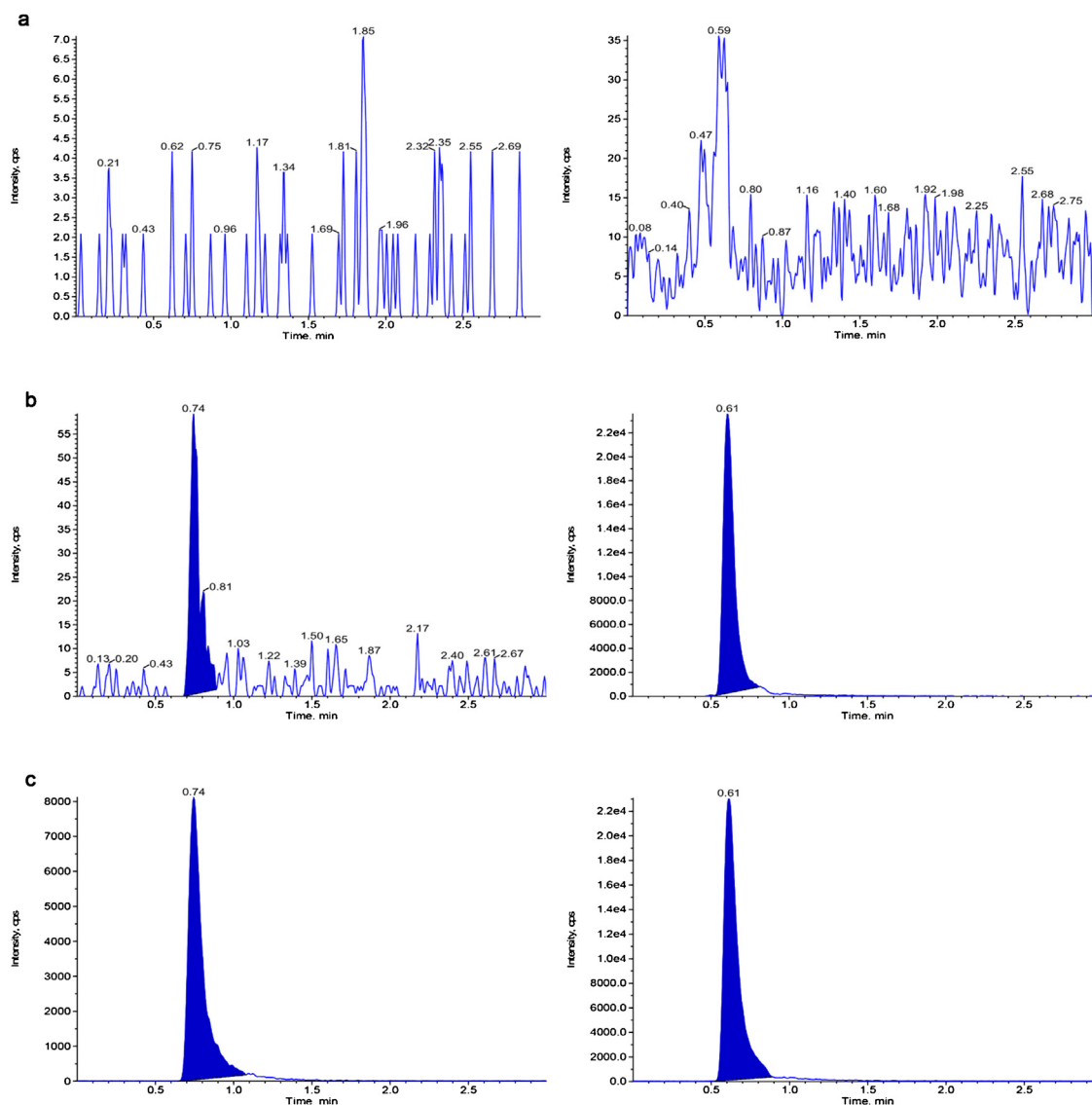


Fig. 2. Liquid chromatography-tandem mass spectrometry chromatograms of motolimid and GS-9620 in rat plasma. (A) Blank rat plasma. (B) Rat plasma containing 1 ng/mL motolimid and 200 ng/mL GS-9620. (C) Plasma sample taken 45 min after intravenous administration of 2 mg/kg motolimid to the rats. LLOQ, lower limit of quantification.

Table 1
Intra- and inter-day precision and accuracy values.

Spiked Concentration (ng/mL)	Measured Concentration (ng/mL)	Precision (%)	Accuracy (%)
Intra-day batch (n = 6)			
1	0.99 ± 0.16	16.3	1.2
3	2.73 ± 0.29	10.6	9.1
100	102.65 ± 6.17	6.0	2.7
900	953.17 ± 45.65	4.8	5.9
Inter-day batch (n = 15)			
1	1.00 ± 0.11	10.7	0.3
3	2.92 ± 0.29	9.8	2.7
100	100.32 ± 4.80	4.8	0.3
900	924.67 ± 50.30	5.4	2.7

for motolimid and GS-9620 from the rat plasma were 109.4 % and 107.5 %, respectively. The efficiency of the protein precipitation was 102.9 % for motolimid and 112.0 % for GS-9620. The results demonstrate that the protein precipitation method used is consistent and practical for the bioanalysis of motolimid and GS-9620.

The results of the stability tests show that motolimid (3 and 900 ng/mL) is stable under the conditions investigated (Table 2).

3.3. Pharmacokinetic studies

The mean plasma concentration-time curves for motolimid after it was orally (0.6 mg/kg) and intravenously (0.6, 2, and 6 mg/kg) administered to the rats are shown in Fig. 3. The pharmacokinetic parameters, as estimated by a standard moment analysis, are listed in Table 3.

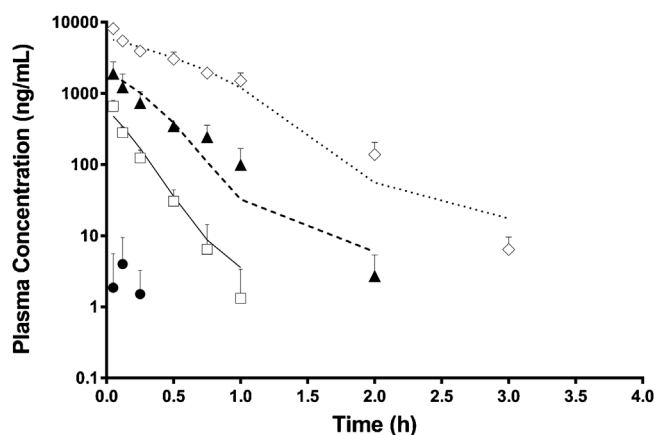
Table 2
Stability of motolimid in rat plasma (n = 4).

Stability Condition	Spiked Concentration (ng/mL)	Measured Concentration (ng/mL)	Relative Concentration (%)
Short-term storage (room temperature for 6 h)	3	3.00 ± 0.34	98.9
	900	834.11 ± 34.77	92.7
Long-term storage (−20 °C for 28 days)	3	3.08 ± 0.35	102.6
	900	916.46 ± 2.78	101.6
Freeze-thaw (3 cycles**)	3	2.83 ± 0.18	94.3
	900	824.46 ± 62.68	91.6
Processed sample (4 °C for 24 h)	3	2.74 ± 0.17	91.3
	900	828.99 ± 96.62	92.1

**Freeze-thaw cycles: −80 °C → RT.

Table 3
Pharmacokinetic parameters obtained by non-compartmental analysis of motolimid after intravenous and oral administration to rats.

Parameter	Intravenous	Oral		
Dose (mg/kg)	0.6	2	6	0.6
T _{max} (h)	0.050 ± 0.000	0.050 ± 0.000	0.050 ± 0.000	0.120 ± 0.000
C _{max} (μg/mL)	0.657 ± 0.138	1.895 ± 0.871	8.136 ± 0.463	0.004 ± 0.005
T _{1/2} (h)	0.110 ± 0.023	0.186 ± 0.020	0.303 ± 0.046	NC
AUC _{0-t} (μg·h/mL)	0.100 ± 0.022	0.586 ± 0.199	4.096 ± 0.613	0.001 ± 0.001
AUC _{0-∞} (μg·h/mL)	0.101 ± 0.022	0.587 ± 0.199	4.099 ± 0.613	NC
CL (L/h/kg)	6.187 ± 1.316	3.728 ± 1.212	1.491 ± 0.231	–
V _{ss} (L/kg)	0.995 ± 0.169	1.379 ± 0.567	0.805 ± 0.082	–
Bioavailability (%)	–	–	–	0.752

AUC, area under the plasma concentration–time curve; CL, systemic clearance; C_{max}, peak plasma concentration; NC, not calculated; T_{1/2}, terminal elimination half-life; T_{max}, time to reach C_{max}; V_{ss}, steady-state volume of distribution.**Fig. 3.** Plasma concentration–time curves after oral (0.6 mg/kg, ●) and intravenous (0.6 mg/kg, □; 2 mg/kg, ▲; and 6 mg/kg, ◇) administration of motolimid to SD rats. Each data point represents the mean ± standard deviation (n = 5). The lines (solid, 0.6 mg/kg; dashed, 0.2 mg/kg; dotted, 6 mg/kg) represent data fitted by the two-compartment model with Michaelis–Menten elimination kinetics.

Following intravenous injection, motolimid showed a typical nonlinear response pattern with an increasing slope as its dose increased. However, following oral administration, most samples except three were below the quantitative limit with very low concentrations compared to the values obtained after intravenous administration. The systemic clearance (CL) values obtained were moderate to high: 6.187 ± 1.316, 3.728 ± 1.212, and 1.491 ± 0.231 L/h/kg for doses of 0.6, 2, and 6 mg/kg, respectively. The CL value for the 0.6 mg/kg dose (i.e., 6.187 L/h/kg) was higher than the normal hepatic blood flow rate in rats (3.3 L/h/kg), which suggests that motolimid possibly undergoes extrahepatic metabolism. The values for the steady-state volume of distribution (V_{ss}) for motolimid after intravenous administration were 0.995 ± 0.169, 1.379 ± 0.567, and 0.805 ± 0.082 L/kg at doses of 0.6, 2, and 6 mg/kg, respectively. The half-life (T_{1/2}) values obtained were 0.110 ± 0.023, 0.186 ± 0.020, and 0.303 ± 0.046 h for doses of 0.6, 2, and 6 mg/kg, respectively, which were relatively short. There were

statistically significant differences in the CL and T_{1/2} values ($p < 0.0001$, one-way analysis of variance [ANOVA]) obtained for the various doses; however, this was not the case for V_{ss} ($p > 0.05$, one-way ANOVA), which indicates that the elimination of motolimid was saturated (Table 3).

In addition, a compartment-based pharmacokinetic analysis was performed for plasma concentration–time profiles after intravenous administration (0.6–6 mg/kg). Among the pharmacokinetic model structures of one- and two-compartment, with or without non-linear elimination kinetics, the two-compartment model with non-linear elimination kinetics was the best to describe the behavior of the plasma concentration–time profiles obtained in this study. Therefore, in this established model, the K_m and V_{max} were estimated to be 770 ng/mL and 5340 ng/mL/h, respectively. k₁₂ and k₂₁ were estimated to be 0.327 and 1.02 h^{−1}, respectively. The fitted plasma concentration–time profiles obtained are shown in Fig. 3 and values for all the parameters were determined simultaneously for all the determinations carried out in this study.

An appropriate elimination phase after oral administration of motolimid to the rats could not be achieved; therefore, the elimination rate constant (k_e), half-life, and area under the plasma concentration–time curve (AUC) from time zero to infinity, AUC_{0-∞}, associated with k_e could not be calculated. The bioavailability estimated by comparing the AUCs from time zero to the last measurable time (AUC_{0-t}) after intravenous and oral administration of motolimid was <1 %. Clinical trials have been performed in which motolimid was administered subcutaneously rather than orally, because of the very low exposure level of motolimid after oral dosing.

To find out whether repeated intravenous administration of motolimid changes the pharmacokinetics of motolimid, rats (n = 4) were administered daily intravenous treatments at 2 mg/kg for 7 days. The CL, V_{ss}, and T_{1/2} values of motolimid after repeated doses administered for 7 days were 2.831 ± 478 L/h/kg, 1.779 ± 289 L/kg, and 0.462 ± 0.088 h, respectively; the respective values for the vehicle-pretreated group were 3.025 ± 1.040 L/h/kg, 1.310 ± 401 L/kg, and 0.371 ± 0.101 h. The CL, V_{ss}, and T_{1/2} values for the repeated-administration group were similar to those for the control group and no significant differences were observed (two-

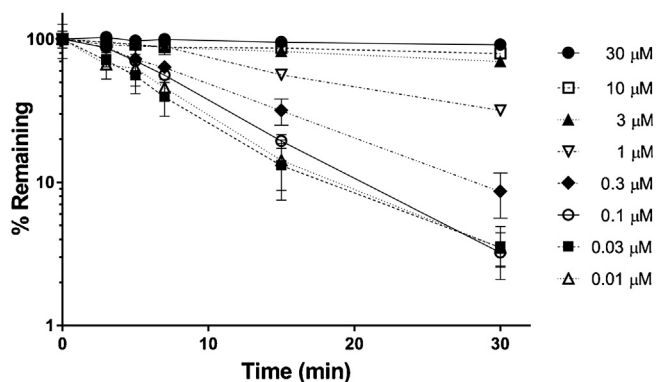


Fig. 4. Profiles showing the percentage of motolimod (0.01–30 μM) remaining in rat hepatic microsomes. Each data point represents the mean \pm standard deviation ($n = 3$).

tailed unpaired t -test: $p > 0.05$), which indicates that motolimod does not possess time-dependent pharmacokinetics after repeated intravenous administration at 2 mg/kg.

The mean remaining-time profiles for motolimod in rat hepatic microsomes are shown in Fig. 4. After a 30-min metabolic reaction of 0.01, 0.03, 0.1, 0.3, 1, 3, 10, and 30 μM motolimod in the liver microsomes, the amounts of motolimod that remained were 3.50 ± 0.94 , 3.51 ± 1.41 , 3.23 ± 0.62 , 8.61 ± 2.99 , 31.78 ± 2.37 , 69.85 ± 4.13 , 79.25 ± 6.07 , and 91.05 ± 7.42 %, respectively. This indicates that low concentrations of motolimod are metabolically unstable. The half-life values calculated from the slopes of the respective curves were 6.09, 6.10, 5.82, 17.36, 60.69, 99.43, and 194.80 min for the 0.01, 0.03, 0.1, 0.3, 1, 3, 10, and 30 μM motolimod concentrations, respectively, showing that the half-life increased from the 0.3 μM concentration; therefore, the value of $\text{CL}_{\text{int, vitro}}$ was calculated from the mean remaining-time profile for 0.1 μM motolimod to be $238.10 \mu\text{L}/\text{min}/\text{mg}$ protein, which is similar to the value ($159.06 \mu\text{L}/\text{min}/\text{mg}$ protein) reported by Zhao et al. [5]. Zhao et al. [5], suggested that motolimod is rapidly eliminated from the body because the “predicted *in vivo* clearance”, which was calculated as “ $\text{CL}_{\text{int, vivo}} \times \text{hepatic blood flow}/(\text{CL}_{\text{int, vivo}} + \text{hepatic blood flow})$ ” was $46.14 \text{ mL}/\text{min}/\text{kg}$. However, we believe that this conclusion might not be rational because the authors did not consider any nonspecific binding in their calculation. To estimate the *in vivo* hepatic clearance, the ratios of microsomal binding to motolimod, plasma protein binding to motolimod, and blood to plasma motolimod concentration were to be 47.99 ± 9.69 , 99.05 ± 0.18 , and 126.58 ± 5.55 %, respectively. Cytochrome P450 (CYP)-mediated unbound hepatic intrinsic clearance ($\text{CL}_{\text{u, int, vivo}}$) was reported to be $824 \text{ mL}/\text{min}/\text{kg}$ in a previous study. Additionally, CL_h of motolimod was estimated to be $5.68 \text{ mL}/\text{min}/\text{kg}$, taking hepatic blood flow ($55 \text{ mL}/\text{min}/\text{kg}$) and the fraction of unbound motolimod in blood (0.75 %) into consideration [13,14]. In the present study, the predicted CL_h was only a small percentage of the *in vivo* systemic clearance (0.341 vs. $6.187 \text{ L}/\text{h}/\text{kg}$), which suggests that CYP-mediated metabolism might not be a major elimination route for motolimod in rats. Therefore, further studies on phase 2 metabolism and/or extrahepatic metabolism of motolimod are needed.

4. Conclusions

A reliable LC–MS/MS method for the quantitation of motolimod in rat plasma was developed and validated. The method provided linearity over a range of 1–1000 ng/mL. An efficient sample

preparation procedure with adequate recovery of motolimod from rat plasma was used with no significant matrix effect. The method was then successfully used in a pharmacokinetic study of motolimod in SD rats. Motolimod showed dose-dependent pharmacokinetics after it was intravenously administered at 0.6–6 mg/kg and very low exposure with an oral bioavailability value of < 1 % in rats. In addition, it showed low metabolic stability in the liver microsomes and extensive binding to the plasma proteins.

Acknowledgements

This research was supported by the Bio & Medical Technology Development Program of the National Research Foundation (NRF) funded by the Korean government (MSIT) (No. 2017M3A9C8021844 and 2015M3A9B5053643).

References

- [1] T. Kawai, S. Akira, The role of pattern-recognition receptors in innate immunity: update on Toll-like receptors, *Nat. Immunol.* 11 (5) (2010) 373.
- [2] X. Han, X. Li, S.C. Yue, A. Anandaiah, F. Hashem, P.S. Reinach, H. Koziel, S.D. Tachado, Epigenetic regulation of tumor necrosis factor alpha (TNF α) release in human macrophages by HIV-1 single-stranded RNA (ssRNA) is dependent on TLR8 signaling, *J. Biol. Chem.* 287 (17) (2012) 13778–13786.
- [3] H. Lu, G.N. Dietsch, M.-A.H. Matthews, Y. Yang, S. Ghanekar, M. Inokuma, M. Suni, V.C. Maino, K.E. Henderson, J.J. Howbert, VTX-2337 is a novel TLR8 agonist that activates NK cells and augments ADCC, *Clin. Cancer Res.* 18 (2) (2012) 499–509.
- [4] R.L. Ferris, N.F. Saba, B.J. Gitlitz, R. Haddad, A. Sukari, P. Neupane, J.C. Morris, K. Misiukiewicz, J.E. Bauman, M. Fenton, Effect of adding motolimod to standard combination chemotherapy and cetuximab treatment of patients with squamous cell carcinoma of the head and neck: the Active8 Randomized Clinical Trial, *JAMA Oncol.* 4 (11) (2018) 1583–1588.
- [5] Z. Li, S. Zhao, Y. Yuan, L. Zhang, Z. Song, X. Tian, X. Zhang, In vitro metabolic profiles of motolimod by using liquid chromatography tandem mass spectrometry: metabolic stability, metabolite characterization and species comparison, *J. Pharm. Biomed. Anal.* (2019).
- [6] H.-C. Hyun, J.-W. Jeong, H.-R. Kim, J.-H. Oh, J.-H. Lee, S. Choi, Y.-S. Kim, T.-S. Koo, Development and validation of a liquid chromatography–tandem mass spectrometry method for the assay of tafamidis in rat plasma: application to a pharmacokinetic study in rats, *J. Pharm. Biomed. Anal.* (2017).
- [7] U. Food, D. Administration, Guidance for Industry: Bioanalytical Method Validation, 2013, 2016.
- [8] C.f.M.P.F.H. Use, Guideline on Bioanalytical Method Validation, European Medicines Agency, 2011.
- [9] J.-W. Jeong, J.-H. Oh, Y.-G. Ji, Y.-M. Shin, M.H. Lee, N.S. Kang, W. Lee, S.-S. Kim, T.-Y. Kim, T.-S. Koo, Liquid chromatography–tandem mass spectrometry of recombinant human extracellular superoxide dismutase (rhSOD3) in mouse plasma and its application to pharmacokinetic study, *J. Pharm. Biomed. Anal.* 164 (2019) 590–597.
- [10] S.-H. Jeong, J.-H. Jang, H.-Y. Cho, I.-J. Oh, Y.-B. Lee, A sensitive UPLC–ESI–MS/MS method for the quantification of cinnamic acid in vivo and in vitro: application to pharmacokinetic and protein binding study in human plasma, *J. Pharm. Investig.* (2019) 1–14.
- [11] M.G. Elhennawy, H.-S. Lin, Dose- and time-dependent pharmacokinetics of apigenin trimethyl ether, *Eur. J. Pharm. Sci.* 118 (2018) 96–102.
- [12] J.-H. Lee, S.H. Ahn, H.-J. Maeng, W. Lee, D.-D. Kim, S.-J. Chung, The identification of lobeglitazone metabolites in rat liver microsomes and the kinetics of the *in vivo* formation of the major metabolite M1 in rats, *J. Pharm. Biomed. Anal.* 115 (2015) 375–382.
- [13] T. Iwatsubo, N. Hirota, T. Ooie, H. Suzuki, N. Shimada, K. Chiba, T. Ishizaki, C.E. Green, C.A. Tyson, Y. Sugiyama, Prediction of *in vivo* drug metabolism in the human liver from *in vitro* metabolism data, *Pharmacol. Ther.* 73 (2) (1997) 147–171.
- [14] B. Davies, T. Morris, Physiological parameters in laboratory animals and humans, *Pharmaceut. Res.* 10 (7) (1993) 1093–1095.
- [15] Y. Lu, N. Zhou, S. Liao, N. Su, D. He, Q. Tian, B. Chen, S. Yao, Detection of adulteration of anti-hypertension dietary supplements and traditional Chinese medicines with synthetic drugs using LC/MS, *Food Addit. Contam.* 27 (7) (2010) 893–902.